An interesting environmental friendly cleanup: the excellent potential of olive pomace for disperse blue adsorption/desorption from wastewater

V. Rizzi[a], F. D'Agostino[a], P. Fini[a,b], P. Semeraro[a,b] and P.Cosma[a,b]*

[a]Università degli Studi "Aldo Moro" di Bari, Dip. Chimica, Via Orabona, 4- 70126 Bari, Italy.

[b]Consiglio Nazionale delle Ricerche CNR-IPCF, UOS Bari, Via Orabona, 4- 70126 Bari, Italy.

Corresponding Author:

Prof. Pinalysa COSMA

Università degli Studi "Aldo Moro" di Bari

Dipartimento di Chimica

Via Orabona, 4

I-70126 Bari, ITALY

e-mail: pinalysa.cosma@uniba.it

tel. +39 0805443443

fax +39 0805442128

ABSTRACT:

The removal of Disperse Blue 73 from aqueous solutions, using olive pomace as adsorbent material, was investigated in a batch system with respect to contact time, pomace dosage, pH and temperature. SEM, FTIR-ATR, TG and XPS analyses appeared as powerful tools to characterize olive pomace, before and after the adsorption of dye, while UV-Visible analyses were used to quantify the amount of loaded dye on adsorbent material. The pseudo-second order kinetic model well fitted the experimental data and described the kinetic adsorption process. The dye desorption in glacial acetic acid was also obtained with the dye recovery enabling the recycle both of adsorbent material and dye itself. Five consecutive cycles of adsorption and desorption were performed and the absence of any degradation process affecting the dye after the adsorption/desorption cycles was observed. The recorded absorption spectrum, in acetic acid solution, before and after the desorption, confirmed such result. An environmentally friendly and a low cost material is thus presented, showing the excellent olive pomace potential both in disperse blue adsorption (with an efficiency of 100%) and desorption (with a mean value of 80% for each cycle). Additionally, an alternative environmental friendly use of olive oil solid residues is presented.

Keywords: Textile dye, Olive pomace, Wastewater treatment, Direct Blue, Dye Removal, Dye Recover

1. Introduction

Over the last few years, the use of dyes, employed for several industrial processes such as paper and pulp manufacturing, plastics, dyeing of cloth, leather treatment and printing has considerably increased. Thus, due to the release of toxic textile dyes in the environment, the life of some organisms is affected with the incidence for aquatic life systems.[1] Moreover, as suggested by Malik[2] and Namasivayam et al.[3], the by-products arisen from dye reactions are highly

carcinogenic and mutagenic. Indeed, the importance of the problem appears more evident considering, in accordance with the Color Index (managed by the Society of Dyers and Colorists and the American Association of Textile Chemists and Colorists), that more than 10,000 types of dyes are available in the world with a mean annual production of over 700,000 tons of dyes.[4] Generally, dyes can be classified as anionic (direct, acid and reactive dyes), cationic (basic dyes) and non-ionic (disperse dyes)[5]. In particular, besides azo-dyes, the anthraquinone dyes, belonging to the disperse ones, represent the second largest class of textile pigments occurring resistant against degradation due to their aromatic structures. Their synthesis is complex and the product costs are higher if compared with azo dyes.[6] Moreover, the degradation efficiency of anthraquinone dyes depends mainly on the microbial capacity to remove chromogenic groups.[7] Thus, it appears clear that scientific communities have the responsibility to contribute to the wastewater treatment with the aim to develop efficient dye removal techniques.[5] Recently, we have shown the excellent ability of cyclodextrins in dyes removal from wastewater.[8] More specifically, anionic azo-dyes (direct) were studied. The use of chitosan films[9] in dye removal from wastewater was also extensively studied, showing an innovative procedures to modify chitosan adsorbent improving the anionic azo-dyes uploading. However, in the point of view of a circular green economy, one of the main objectives is also the reuse of both the adsorbent materials and dyes. In fact, the latter purpose represents another important topic of research beside the "simple" removal of dyes from wastewater with the possibility to perform many cycles of dye adsorption/desorption, reducing at least the cost as a whole. Excellent results were obtained, for anionic dyes, considering, for example, the use of cyclodextrins.

In this paper, the attention was focused on the anthraquinone dye, Disperse Blue 73 (DB), as an example of disperse dye. An innovative material, the olive pomace (OP), as a physical adsorbent was used enabling the possibility to recover the disperse dye for several textile dyeing processes. Indeed, among treatment technologies, the adsorption has rapidly gaining importance as a method for aqueous effluents treatment. Not surprisingly, some of the advantages of adsorption process are

the promising low cost regeneration of the adsorbent, the availability of known process equipment, simple operations and recovery of the adsorbed compounds.[10] Further, the agricultural waste materials have little or no economic value and often induce a discarding problem. Therefore, the use of agricultural wastes can be considered of great significance for our purpose.[5] With this regard, The European Union is the main producer and consumer of olive oil in the world. Indeed, recently, in the 2014, Bhatnagar et al.[11] reported that the global olive oil production for 2010 was estimated to be 2,881,500 metric tons. Moreover, the worldwide consumption of olive oil is increased of 78 % between 1990 and 2010. Valta et al.[12] (2015) reported an increase of this production reaching the value of 3.3 million tons for the 2011/2012. The increase in olive oil production implies a proportional increase in olive mill wastes[11] and the main world producer countries are reported to be Spain, Italy, Greece, Turkey, Syria and Tunisia.[13] Indeed, olive production across the Mediterranean area has a long and prestigious past and nowadays the olive oil industries are very important in Mediterranean countries, both in terms of wealth and tradition.[14] Consequently, this area is affected by olive mill wastes pollution and many efforts are attempted to overpass this problem with innovative technologies.[15] As a consequence of such increasing trend, olive solid residues are facing severe environmental problems due to lack of feasible and/or cost-effective solutions to olive waste management.12 For this reason, among biomaterials, solid residues of the olive oil production could constitute a promising low-cost adsorbents[16] overcoming two problems: the elimination of olive solid residues from environment, in order to use the latter to reduce another important class of pollutants, i.e. dyes from wastewater. Not surprisingly, some of these olive oil wastes were tested as low cost biosorbents materials for several pollutant disorders.[17] Olive pomace consists of cellulose, lignin, amino acid, protein, uronic acids and polyphenolic compounds and it is generally swallowed by means of controlled spreading on agricultural soil and only a small amount of this residue is used as natural fertilizer, or as source of heat energy or as additive in animal food.[18] One of the interesting use of such olive solid wastes is to remove mainly heavy metals from water. For example Lead,

Chromium, Cadmium, Zinc, Nickel, Copper, Arsenic Mercury and Iron are reported as metals extensively studied in literature.[11] Starting from 1998, the potential use of processed solid residues of olive mill products to treat drinking water containing several heavy metals in trace concentrations was explored.[19] Successively, the studies about the possible use of olive mill solid wastes as a low cost remediating adsorbent for heavy metals biosorbents, raised[16,20-24]. However, although a thorough literature survey indicates that pomace waste, or their derivatives, were used as adsorbent for removing heavy metals, its use as dye adsorbent from wastewater is limited. Indeed, to our knowledge, olive pomace was only used, from 2000 to nowadays, to prepare active carbon as adsorbent to remove different dyes.[25--34] With regard the use of olive pomace without further modifications, Banat et al.[35] presented the removal of Methylene Blue dye from aqueous solutions by olive pomace showing that the dye uptake increased with the increase of OP amount reaching the equilibrium within 7 h. Akar et al.[18] reported dye biosorption potential of untreated olive pomace showing interesting results especially at acid pH values. Clearly in the olive pomace-related literature a gap is present when the material, as it is, without further treatments, is used for dye removal from wastewater. The presence of this gap is further confirmed by Anastopoulos et al.[36] (2015) which describe the use of residues and by-products of the olive-oil production chain for the removal of pollutants from environmental media, showing as the olive pomace is extensively used for heavy metal removal with a reduced number of manuscripts related to dyes adsorption. Starting from these considerations, in this study, olive pomace has been chosen as adsorbent material for removal and recovery, for the first time, of a disperse dye from wastewater exhibiting excellent performance with a very fast adsorption and desorption. DB is chosen as a model dye testing, in accordance with several publications,[37-39] the upload ability of olive pomace in the same conditions of industrial textiles dyeing processes: i.e. from aqueous/acetic acid DB solutions, pH 3.5, as suggested by Colorprint Fashion, a Spanish textile industry.

2. Material and Methods

All the chemicals used were of analytical grade and samples were prepared using double distilled water. Acetic acid (99,9 %), NaOH and HCl was purchased from Sigma-Aldrich. Disperse Blue 73 was received by Colorprint Fashion, S.L within the LIFE+ European Project named "DYES4EVER" (Demonstration of Cyclodextrin Techniques in Treatment of Waste Water in Textile Industry to Recover and Reuse Textile Dyes) and used without further purification. DB stock solution with a concentration of 1×10^{-4} M was prepared in double distilled water containing 500µL of acetic acid (from a 80% stock solution) per liter of solution for mimicking the textiles dyeing conditions (proposed by Colorprint Fashion). Dilutions in double distilled water were obtained. When necessary, the pH of the various aqueous solutions was adjusted using concentrated HCl (0.5M) and NaOH (1M) solutions.

2.1 Disperse Blue information:

Color Index Number: 73; chemical formula: $C_{20}H_{14}N_2O_5$; MW: 362.34 g mol^{-1} (see **Scheme 1**).

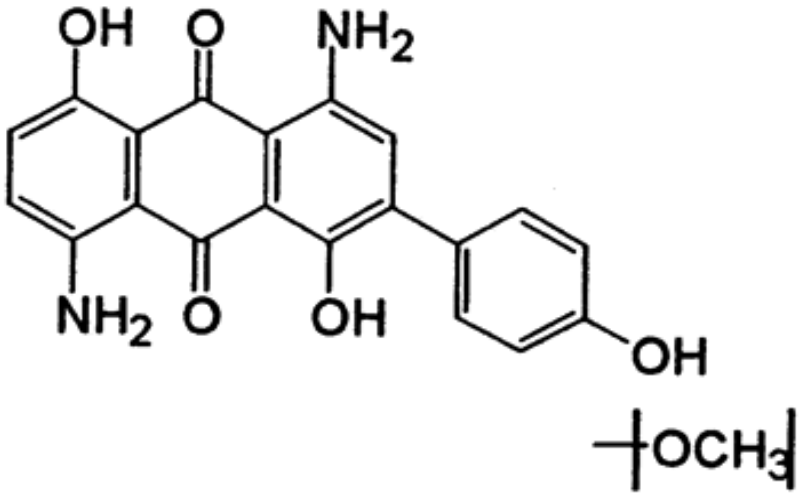

Scheme 1: Chemical structure of disperse blue 73

2.2 Biosorbent Preparation

Biosorbent material was the solid waste of olive oil production, provided from local oil industry, Bari, Italy. The sample was repeatedly washed with deionized water, at 100 °C (until clean water was obtained), in order to remove adhering dirt and soluble impurities and, then, dried at 100 °C in an oven until constant weight. The sample was used both as obtained after the treatment (OP a.t.) and also crushed and sieved (OP_P a.t.). OP a.t. and OP_P a.t. biosorbents were stored in a glass bottles prior to use.

2.3 Experimental procedures

Batch experiments were conducted in 40 mL glass beakers containing known concentrations of DB solutions. With the aim to check the effect of the biosorbent and DB dosage on dye molecules removal from wastewater, the biosorbent amount was changed between 0.25 and 3.00 g and the DB concentrations were settled at 5×10^{-5}M, 8×10^{-5}M and 1×10^{-4}M. Measurements were performed in the adopted volume and at the pH of acid DB solution, i.e. 3.5 units. The biosorption kinetics of DB was examined at constant temperatures of 25, 50 and 100°C, however the adsorption occurred only a 100°C due to the absence of results at lower temperatures. The effect of pH on the biosorption process was also evaluated removing acetic acid from DB solution, obtaining, thus, a neutral solution (pH 6.6) and at least, OP a.t and OP_P a.t. were washed with an appropriate amount of NaOH in order to charge, negatively, the surface of the adopted material. The mixtures were stirred at 140 rpm for different contact times using a digitally controlled magnetic stirrer. With regard to the adsorption process, the DB UV-Vis absorbance value at 530 nm was used, in conjunction with the analytical concentration of dyes (5×10^{-5}M, pH 3.5), with the aim of estimating the molar absorption coefficients (ε). The obtained value, expressed in $M^{-1}cm^{-1}$ units, was: 4000. This ε value was used to determine the DB concentration at several contact times with olive pomace. When the desorption process was considered, the same approach was used, following the DB UV-Vis absorbance value at 622nm, in acetic acid. 10400$M^{-1}cm^{-1}$ was used as

molar absorption coefficients at this wavelength. In accordance with several studies reported in literature[8,9,38] and related to dye adsorption from wastewater, the adsorption capacity q_t (mg×g^{-1}) at time t of DB, was calculated by applying the following equation (Equation 1):

$$q_t = \frac{C_0 - C_t}{W} \times V \qquad \text{Equation 1}$$

where V represents the adopted total volume of solution (herein 40 mL), W is the weight of the dry adsorbent material (g), C_0 and C_t represent the initial concentration and the concentration at time t of the dye (mg L^{-1}).[8,9]

2.4 Adsorption kinetics

Among different methods proposed in literature to fit experimental kinetic data, the pseudo-first and second order kinetic models are, usually, used to give more information about the dye adsorption kinetics. If on one hand, the Lagergren linear form equation, describing the pseudo-first order model, is well presented by the following relation (Equation 2)[9]:

$$\text{Log}\,(q_e - q_t) = \text{Log}\,q_e - \frac{k_1}{2.303} \qquad \text{Equation 2}$$

where q_e and q_t represent the adsorption capacities at equilibrium and at time t, respectively (mg g^{-1}) and k_1 the rate constant of pseudo-first order adsorption (L min^{-1}); on the other hand the pseudo-second order rate equation of McKay is represented by the following form (Equation 3)[37,39]:

$$\frac{t}{q_t} = \frac{1}{k_2 q_e^{\,2}} + \frac{1}{q_e} \times t \qquad \text{Equation 3}$$

where q_e is the equilibrium adsorption capacity and k_2 (g (mg min)$^{-1}$) the pseudo second-order constants. The latter is easily determined from the slope and intercept of the plot t/q_t versus t. In

this work, these two models were adopted with the aim to describe the adsorption process of DB on olive pomace, searching and showing the best one describing the process.[38]

2.5 UV-Visible and FTIR-ATR spectroscopic measurements

UV-Vis absorption spectra were recorded using a Varian CARY 5 UV-Vis-NIR spectrophotometer (Varian Inc., now Agilent Technologies Inc., Santa Clara, CA, USA). FTIR-ATR spectra were recorded within the 600–4000cm^{-1} range using an Fourier Transform Infrared spectrometer 670-IR (Varian Inc., now Agilent Technologies Inc., Santa Clara, CA, USA), whose resolution was set to 4 cm^{-1}. 32 scans were summed for each acquisition.

2.6 X-ray Photoelectron Spectroscopy (XPS) analysis

XPS analyses were performed using a Thermo Electron Theta Probe spectrometer equipped with a monochromatic Al Ka X-ray source (1486.6eV) operated at a spot size of 300 μm corresponding to a power of 70 W. Survey (0–1400eV) and high resolution (C1s, O1s, N1s) spectra were recorded in FAT (fixed analyzer transmission) mode at pass energy of 200 and 100eV, respectively. All spectra were acquired at a take-off angle of 37° with respect to the sample surface. Charge compensation was accomplished by a low energy electron flood gun (1 eV). Charge correction of the spectra was performed by taking the hydrocarbon (C-C, C-H) component of the C1s spectrum as internal reference (binding energy, BE = 285.0eV). Atomic percentages were calculated from the high resolution spectra using the Scofield sensitivity factors set in the ThermoAvantage V4.87 software (Thermo Fisher Corporation) and a non-linear Shirley background subtraction algorithm. The best-fitting of the high-resolution XPS spectra was performed using with mixed Gaussian-Lorentzian peaks after a Shirley background subtraction; a maximum relative standard deviation of 10% was estimated on the area percentages of the curve-fitting components, while the determined standard deviation in their position was ± 0.2eV.

2.7 Scanning Electron Microscopy (SEM)

The surface morphology of olive pomace was investigated using FEI Quanta FEG 250. Samples were placed on an aluminum stub.

2.8 Thermogravimetry analysis (TGA)

TGA were performed using STA 449 F1 Jupiter, Netzsch apparatus. The samples were analyzed in the range 25-550°C at the heating speed of 3°C min^{-1} and in air atmosphere.

3. Results and Discussion

As a preliminary step of this study, the camera pictures of unloaded OP a.t., related to different magnifications were acquired (Figures 1A and B).

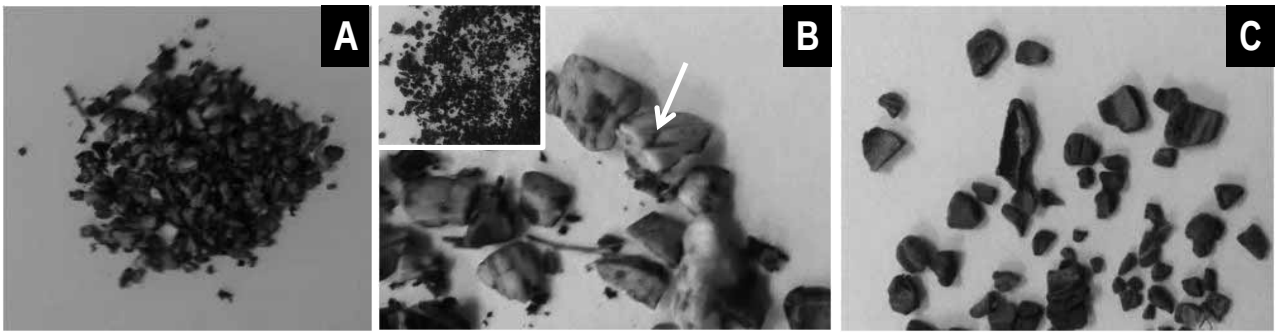

Figure 1: OP a.t camera pictures (A) with related magnification; *inset:* OP_P a.t. (B); OP a.t. loaded with DB dye molecules (C).

The picture, reported as inset in Figure 1B, is related to unloaded OP_P a.t. Clearly, the direct observation of this biomass indicates the heterogeneity of our sample with the presence of macroscopic cavities, as indicated by the white arrow in Figure 1B, potentially able to absorb dye molecules. Indeed, Figure 1C depicts the excellent performance of OP a.t. for the dye adsorption from aqueous solution (water/acetic acid, pH 3.5) having a concentration of 5×10^{-5}M (volume 40mL) at 100°C. As appears from Figure 1C, in which an evident blue colored OP a.t. can be observed, the loaded adsorbent occurs with an homogenous distribution of DB molecules on the material surface itself and, more specifically, the dye molecules appear to fill the macroscopic

cavities, observed in Figure 1B. This result, in terms of adsorption ability, was further emphasized from the direct observation of DB water/acetic acid solution before and after the contact with olive pomace.

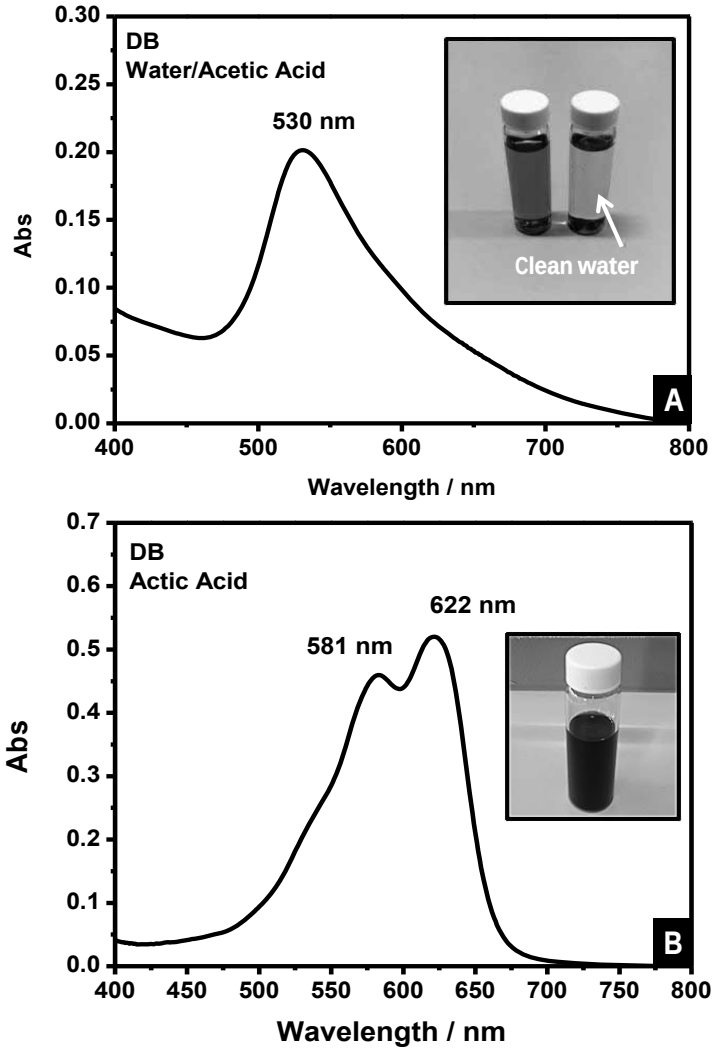

Figure 2: UV-Vis absorption spectrum in pH 3.5 aqueous/acetic acid solutions at 5×10^{-5}M of DB; *inset*: DB solution camera picture, with OP, before and after the adsorption process (A); UV-Vis absorption spectrum in glacial acetic acid solutions at DB 5×10^{-5}M; *inset*: DB solution camera picture (B).

The Figure 2A inset shows the obtained results. The same considerations can be applied to OP_P a.t. With the aim to clean water/acetic acid solution from DB dyes, at initial concentration of 5×10^{-5}M

pH 3.5, using an appropriate amount of olive pomace, different temperatures were examined, i.e. 25, 50 and 100°C; however, only 100°C occurred as the powerful temperature. These data were very interesting since the dyeing industrial processes are performed at high temperatures and we have obtained optimal results, in term of the dye adsorption, in the same conditions in which textiles are dyeing, producing hot colored wastewater. Not surprisingly, as well described recently by Seow et al. (2016)[40], the temperature plays a key role in the adsorption processes and it can be considered as an indicator of the exothermic or endothermic character of the process. The Authors reported that if the adsorption is an endothermic process, the adsorption capacity increases with increasing temperature and this could be mainly ascribed to the increase of the active sites number and the dye molecules mobility under these conditions. Interestingly, in a study related to active carbon, prepared from male flowers coconut tree, used as adsorbent material to remove Cristal Violet, Senthilkumaar et al. (2006)[41] concluded that when the temperature was increased the swelling effect within the internal porous structure of the carbons, enabled more dye molecule diffusion into carbon itself. Additionally, since DB, as disperse dye, is scarcely soluble in water, an high affinity with the adsorbent surface was expected.[42] So, the effect of the dye low solubility, together with the swelling effect of the internal structure of olive pomace and the increased mobility of molecules, enhances the adsorption process, at high temperature, increasing at least the affinity with the adsorbent material. From a quantitative point of view, UV-Vis spectroscopy was used to evaluate the amount of DB in solution during the adsorption and desorption processes. If on one hand, the intensity value registered at the maximum of absorption band (530nm) observed in Figure 2A was followed as function of time to study the dye-uptake from water, on the other hand the absorbance value registered at 622nm (Figure 2B) was used to evaluate the dye release when acetic acid solution was added to loaded olive pomace. As it is possible to see in the inset of Figure 2A, DB water/acetic solution appears with a magenta color that changes to a brilliant blue, when the adsorption on olive pomace occurred (Figure 1C). Moreover, if the DB was dissolved in pure

acetic acid solution (absorption spectrum in Figure 2B), solvent used to desorb the dye, changes in wavelength position occurred due to change in dye solution color (inset in Figure 2B).

3.1 Scanning Electron Microscopy analyses (SEM)

Olive pomace was analyzed by scanning electron microscopy in order to examine carefully its morphology. Interestingly, SEM images of unloaded biomass, with different magnifications, shown in Figure 3A-F, indicate the porous structure of such a biomass.

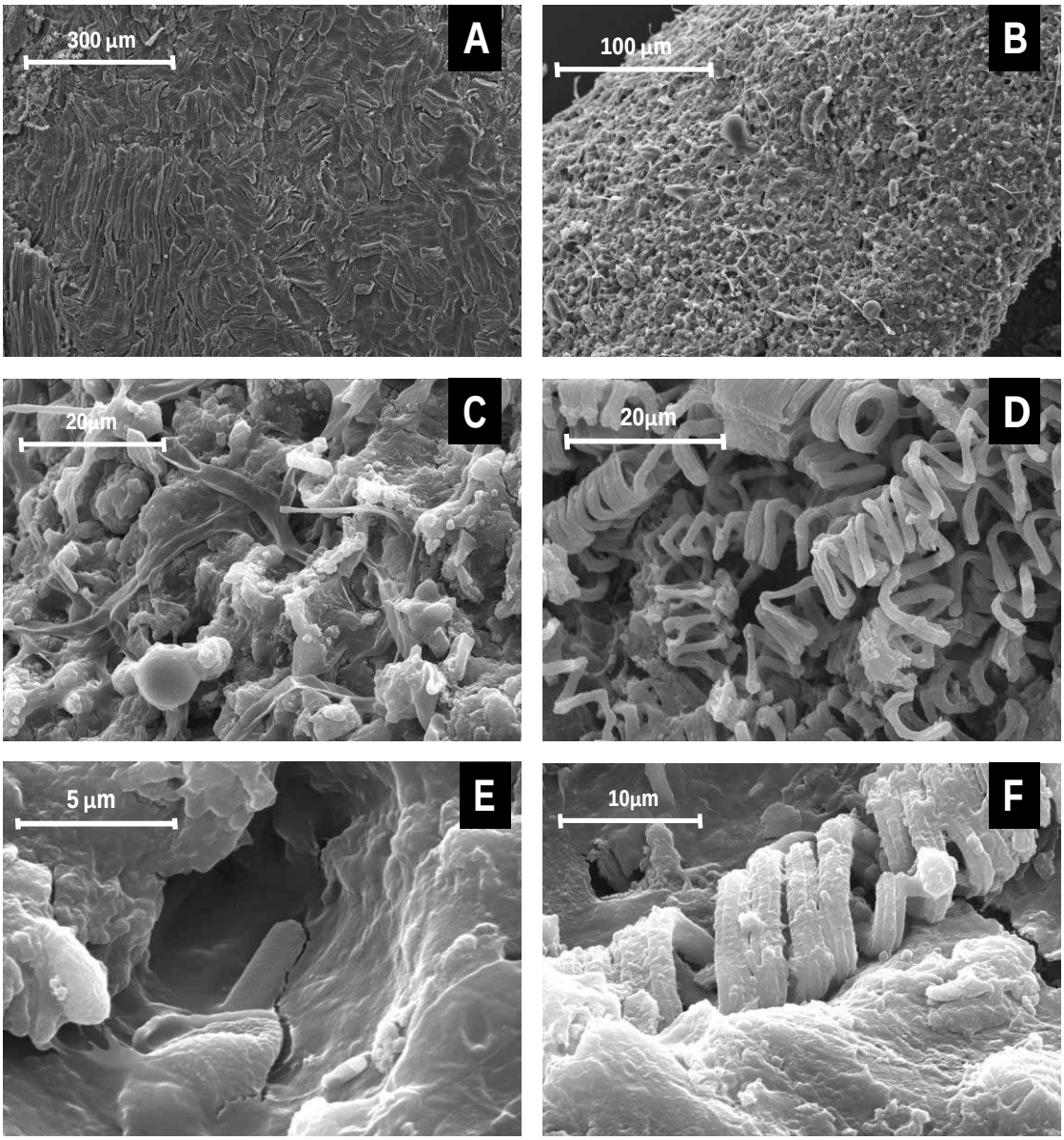

Figure 3: OP SEM images at different magnifications.

Not surprisingly, as already seen from the sample macroscopic investigation, the biosorbent showed some irregular structures (Figure 3C and D with a detailed view in Figures 3E and F) and cavities on the external surface potentially able to adsorb the DB molecules. The analysis highlights the presence of structural features of OP a t./OP_P a.t., very important in increasing the total surface area.[18] However, it is worth mentioning that, as expected, with regard to OP a.t. and OP_P a.t., significant differences were absent, and the samples appeared very similar to each other as a whole. Moreover, the presence of loaded dye molecules did not affected significantly the morphology of the samples.

3.2 FTIR-ATR spectroscopic measurements

In order to better understand the molecular organization of DB inside olive pomace cavities, FTIR-ATR analyses were performed on unloaded and loaded olive pomace. The results, related to OP_P a.t, that occurred to be the same for OP a.t and OP (*data not shown*), are reported in Figure 4.

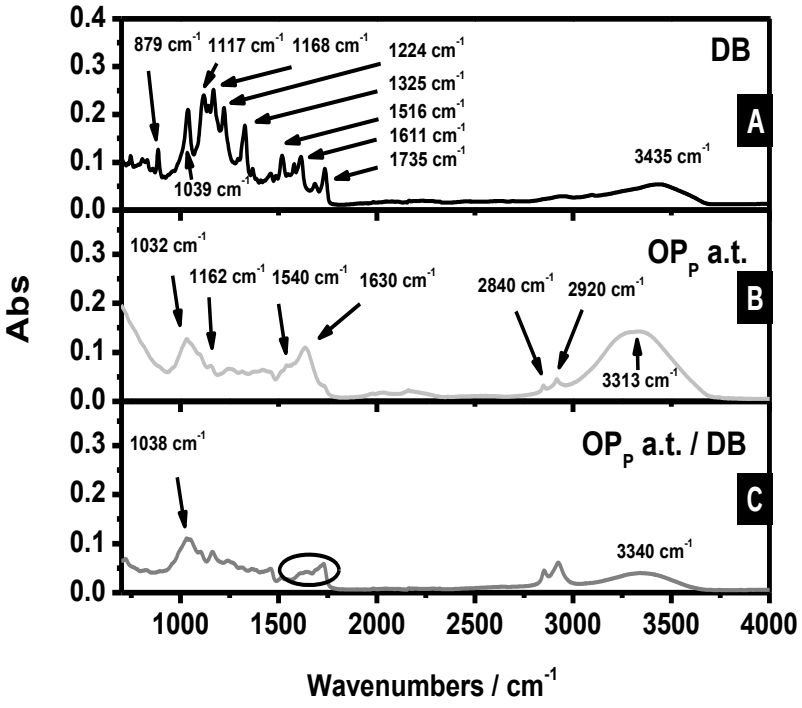

Figure 4: FTIR–ATR spectra in the range: 600-4000 cm^{-1} of DB (A); of OP_P a.t. (B) and of OP_P a.t./DB composite material (C).

The FTIR spectrum of unloaded olive pomace, in the range of 600–4000cm^{-1}, is shown for detecting the incidence of functional groups present on the surface of biosorbent and is reported in Figure 4B. In accordance with Akar et al. (2009)[18], the obtained spectrum suggests the complex nature of the unloaded olive pomace characterized by peculiar vibration modes. As expected, since the nature of our biological material, bands were detected in the wavenumbers region between 3600-2800cm^{-1} and 800-1800cm^{-1}. More specifically, the signal centered at 3313cm^{-1} was ascribed to the overlap of hydroxyl and amino groups stretching present on olive pomace surface. Bands at 2920cm^{-1} and 2840cm^{-1} were observed and were assigned to C-H bonds stretching of methyl and methylene groups present in the lignin structure[18] and generally ascribed to aliphatic compounds.[17] Peaks at 1540cm^{-1} and 1630cm^{-1} were attributed to amino and carboxyl groups stretching, respectively. In the region 900-1200cm^{-1}, bands (at 1032cm^{-1} and 1162cm^{-1}) were detected indicating the presence of saccharidic like-structures, i.e. cellulose and hemicellulose yet suggested by the intense band detected at 3313cm^{-1}.[49] The presence of alcoholic compounds, i.e. phenols and polyphenols was also suggested.[50] The broadened and not well defined bands observed in the region between 1100–1500cm^{-1}, as suggested by Omar et al. (2013)[50] were assigned to CH_3, $–CH_2–$, C–H moieties and to polyphenolic aromatic ring C–C stretching of lignin and, as reported by Martín-Lara et al.(2009)[17], the contribute of bending vibration of O–H bonds, typical for celluloses, can be considered. Additionally, the same Authors[49] at 1318cm^{-1} and 1241cm^{-1} observed the C–O vibrations in carboxylate groups and the stretching of esters (R–CO–O–R′), ethers (e.g. R–O–R′) or phenol groups.[21] Thus, from FTIR interpretation of the olive pomace spectrum arises that the biosorbent matrix consists mainly of cellulose, hemicelluloses and lignin (both hemicellulose and lignin contribute with the higher content of C=O groups) with the presence of amino acids and/or proteins (amino groups). Lignin can be considered the cementing matrix that holds cellulose and hemicellulose units together.[24] The presence of the dye, as reported in Figure 4C, affected the olive pomace spectrum and the results were very similar to those obtained by Akar et al. (2009):[18] (i) the broad O-H and N-H band shifted from 3313cm^{-1} to

3340cm^{-1} decreasing significantly its intensity, (ii) the signal at 2920 and 2840cm^{-1} increased their intensities due to the biosorption of reactive dye molecules including C–H groups in its chemical structure, (iii) the carboxyl and amino groups vibration modes, at 1540 and 1630cm^{-1}, significantly decreased their intensities (black circle in Figure 4C), (iv) the signal at 1032cm^{-1} moved toward higher wavenumbers values, i.e. at 1038cm^{-1}. All of these observations suggested the presence of interaction between DB and olive pomace, via hydrogen bonds and Van der Waals forces, favored by the planar structure of dye, involving hydroxyls and/or ketons, amino moieties and aromatic residues both of adsorbent material and DB molecules (i-iii). The interaction with cellulose or cellulose-like structure was thus suggested (iv) (Timofei et al., 2000). Not surprisingly, disperse dye is used to color cellulose fibers.[6,51] It is worth mentioning that despite results reported by Akar et al. (2009)[18], in which a negatively charged direct dye (RR198) was object of study, in our investigation, DB dye was positively charged since the presence of protonated primary amino groups, under our experimental conditions. However, a negatively charged cloud on anthraquinone residue was also considered. As a result, slight electrostatic interactions could be also considered involving the C=O moieties and/or the anthraquinone residue present on DB structure and protonated amino groups on olive pomace surface. In particular, dipole-charge interaction and viceversa between protonated amino groups present on DB structure and negatively charged moieties present on olive pomace surface (i and iii) could occur. However, the presence of Van der Waals forces, hydrophobic interactions and H-bonds can be considered as the main forces. Indeed, disperse dyes have a hydrophobic character with an expected low aqueous solubility. Timofei et al. (2000)[51] suggest that dyes form charge transfer complex through a donor-acceptor proton complex in cellulose binding. Isa et al. (2007)[52] described an higher affinity for solid surfaces than for water. As the solubility of disperse dyes in the aqueous solution is low, they have a tendency to accumulate at the surface of adsorbents. Thus, as in our condition, the adsorption capacity would increase if the solubility of the dyes is low. Our hypothesis was further confirmed observing the DB i.r. spectrum reported in Figure 4A. Interestingly, when the composite OPP

a.t./DB was considered (Figure 4C) the i.r. bands of DB, reported in Figure 4A, were not detected. Indeed, when only the DB was considered, bands were observed at 1435cm^{-1} (-OH, -NH), 2850-2950cm^{-1} (-CH3), 1735cm^{-1} (C=O), 1600-1425cm^{-1} (C=C, anthraquinone ring), 1224cm^{-1} (C-N), 879cm^{-1} (C–H out-plane bending vibration, anthraquinone ring) and in the region 1000-1200cm^{-1} (C-H in-plane bending vibration, anthraquinone ring).[45] The results indicated that the dye molecules were blocked inside olive pomace matrix deshielding them from detection.

3.3 XPS analyses

XPS atomic percentages of OP_P, OP_P a.t. and OP_P a.t./DB are reported in Table S1, S2 and S3, respectively. The similar XPS atomic percentages were detected for OP and/or OP a.t. in the same experimental conditions. As a whole, if results related to OP_P and OP_P a.t. are compared, the absence of significant variations were observed, in term of BE and composition, in the XPS C1s, O1s and N1s. A slight reorganization of the surface components could be supposed. The major signal observed at 284.8eV suggests the main presence of C-(C,H) moieties, with the partial contribute at higher BE of the C-OH groups, confirmed also by the high percentage of O1s.[53] The adventitious hydrocarbon contamination at this BE was also considered. As a consequence, in agreement with FTIR-ATR measurements and literature,[53] results confirmed the main presence of lignin with the contribute of cellulose and/or cellulose-like structures, i.e. hemicellulose. The presence of fatty acids can be also considered.[54] Moreover, the N1s signal detected at 399.41eV was ascribed to the presence amino acids an proteins.[55] Interestingly, after the treatment with water the same signal shifted from 399.41eV to 401.44eV suggesting the protonation of primary amines on the surface of olive pomace.[56]

When the presence of DB was considered, variation in the OP_P a.t. XPS C1s, O1s and N1s percentages were observed; in particular the considerable increase of the peak area percentage of the hydrocarbon component at 284.8eV was ascribed to DB presence and, specifically, to contributions from the CH_3 moiety and aromatic carbon atoms of the anthraquinone residue. Noticeably the N1s of the OP_P a.t./DB showed also an increased percentage area due to the presence

of amino groups of dye. Interestingly, the expected increase percentage area of the O1s signals, due to C=O of DB, was not observed and the ratio between the peak area percentages of the N1s and O1s increases from 0.049, as observed for OP_P a.t., to about 0.09 in the case of OP_P a.t/DB; this confirm, in excellent agreement with the so far discussed hypothesis, a rearrangement of the olive pomace components induced by DB incorporation suggesting a novel disposition of both the oxygen and amino groups on the olive pomace surface and DB arising from novel coordination. Moreover, the N1s signal shifted to lower BE value as for the signal related to protonated amino groups disappeared. The result suggested, also, the presence of slight electrostatic interactions involving the positively charged amino groups present on olive pomace surface and DB. It worth mentioning that since the reported surface composition of olive pomace, in which the great contribute was ascribed to lignin and cellulose/hemicellulose, the presence of electrostatic interaction involving protonated amino groups, yet discussed during FTIR-ATR analyses, may scarcely contribute to the interaction.

3.4 Thermogravimetric analyses (TGA)

Figure 5A and 5B shows TG and DTG curves of raw and washed olive waste evaluating also the effect induced by the loaded dye molecules. If on one hand, in TGA an appropriate amount of the sample is heated at a specific heating rate and is monitored as a function of time or temperature, on the other hand the first derivative of the curve obtained from the TGA, which is known as "derivative thermogravimetry" (DTG), gives the maximum reaction rate. Generally, an observed maximum in the DTG curve corresponds to a point inflection in the TGA curve at which mass is lost most rapidly.[57] In our study, the typical curves of solid fuel, with several weight loss, were observed. Starting from the "as received" olive pomace, OP_P (Figure 5, black curve) the process started with the evaporation of free moisture content. As the temperature was further increased, the water in the lignocellulosic material also evaporated. Interesting major weights losses were observed in the temperature range between 200 to 400°C and 410 to 500°C and were attributed to

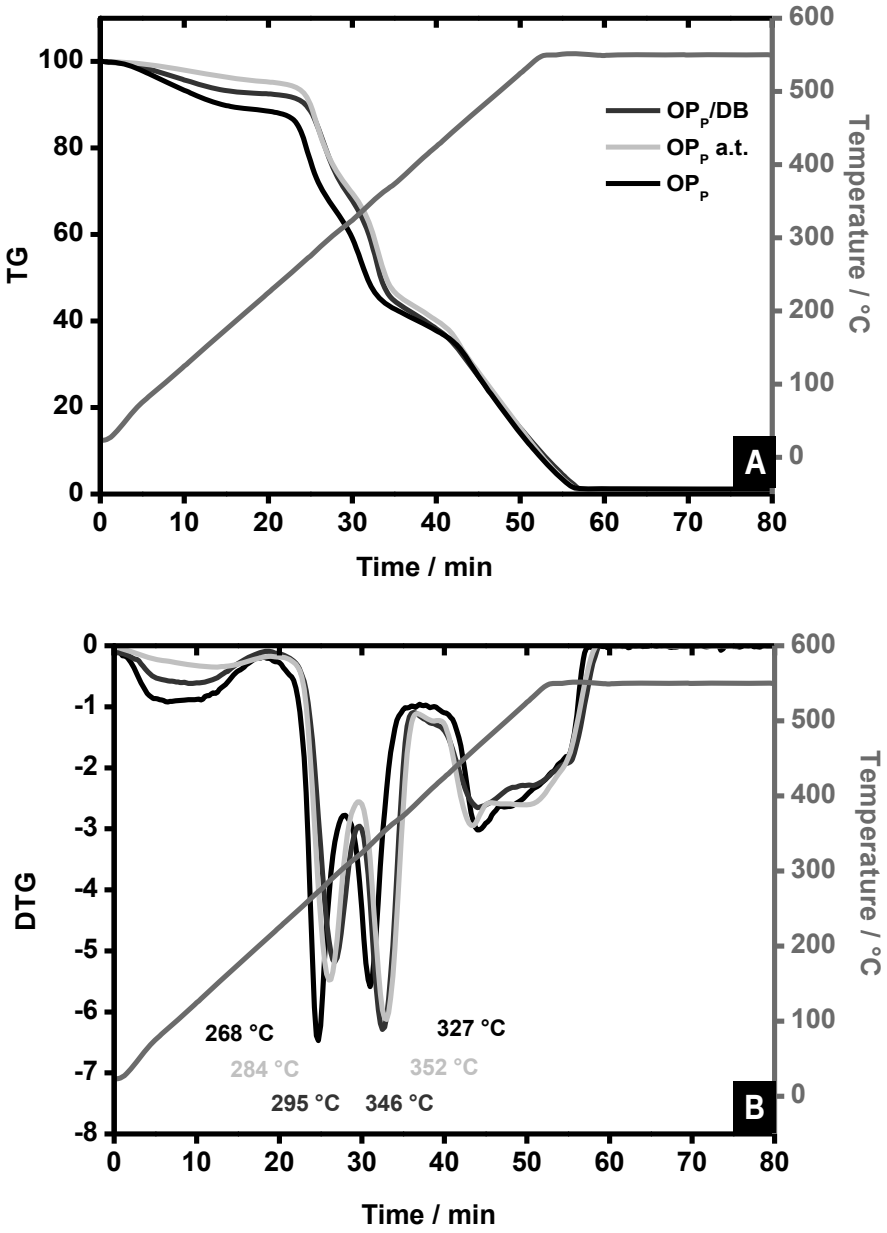

Figure 5: Thermogravimetric analyses (TG): OP_P (Black line), OP_P a.t. (gray line) and OP_P a.t./DB composite material (blue line) (A); Differential Thermogravimetric analyses (DTG) of the same samples (B).

hemicellulose degradation and cellulose and lignin decomposition and to the complete combustion of residues (as a continuation of the slow degradation of lignin), respectively.[50,58,59] Tawarah et al. (2013)[58] assessed that the hemicellulose degradation occurs between 200 and 350°C with maximum rate of degradation at 269°C (as observed in our condition), while cellulose degradation

starts above 320°C. With regard to lignin, Kabakci et al. (2013)[57] reported that the decomposition starts around the temperature of hemicellulose degradation and continued up to 600°C. Interestingly, when OP_P a.t. was considered (Figure 5, gray line) beside the expected reduced weight loss due to the loss of water soluble compounds, the treatment induced a gain in the so far discussed temperatures of degradation of compounds detected in olive pomace matrix. Indeed, the degradation of hemicellulose and cellulose shifted from 268°C to 284°C and from 327°C to 352°C, respectively with variations observed also in tail of the curve indicating that the process affected also the lignin decomposition temperature. Additionally, the treated sample exhibited a rate of weight loss slower than one observed for OPP. When the loaded OPP a.t. was considered (Figure 5, blue curve) a similar scenario occurred with a gain for the temperature of degradation of hemicellulose (shifted from 284°C to 295°C) and a loss for the temperature of degradation of cellulose (shifted from 352°C to 346°C). Once again, in this case, the tail of the curve was affected. Globally the obtained results suggested that DB molecules interacted especially with cellulose and hemicelluloses and lignin, retarding their degradation exhibiting a protective role from oxidation for hemicellulose and lignin. In other word different structures/arrangements were adopted by polymers. The results, once again are in excellent agreement with XPS and FTIR-ATR analyses.

3.5 Effect of adsorbent dosage and dye concentration

The influence of the amount of OP a.t. and OP_P a.t. on DB adsorption, with the related contact time, are shown in Table S4. Clearly, at constant concentration of DB, 5×10^{-5}M, by increasing the adsorbent amount from 0.25 to 3.00g in 40mL of dye water/acetic acid solution, the contact time necessary to adsorb the dye, with an efficiency of 100%, decreased both for OP a.t. and OP_P a.t.. More specifically, excellent performances were obtained powdering the olive pomace. For example, only 3 minutes were necessary to remove completely the dye if 3.00g of OP_P a.t. was used. On the other hand, in the same condition, 8 minutes were enough to obtain the same result using OP a t. Differences between OP a.t. and OP_P a.t. were better emphasized reducing the total amount of the adsorbent material (Table S4). After this assessment the q_t values were calculated both for OP a.t.

and OP_P a.t., and those related to OP_P a.t. are shown in Figure 6A (the same trend was observed for OP a.t. yet elapsing the contact time).

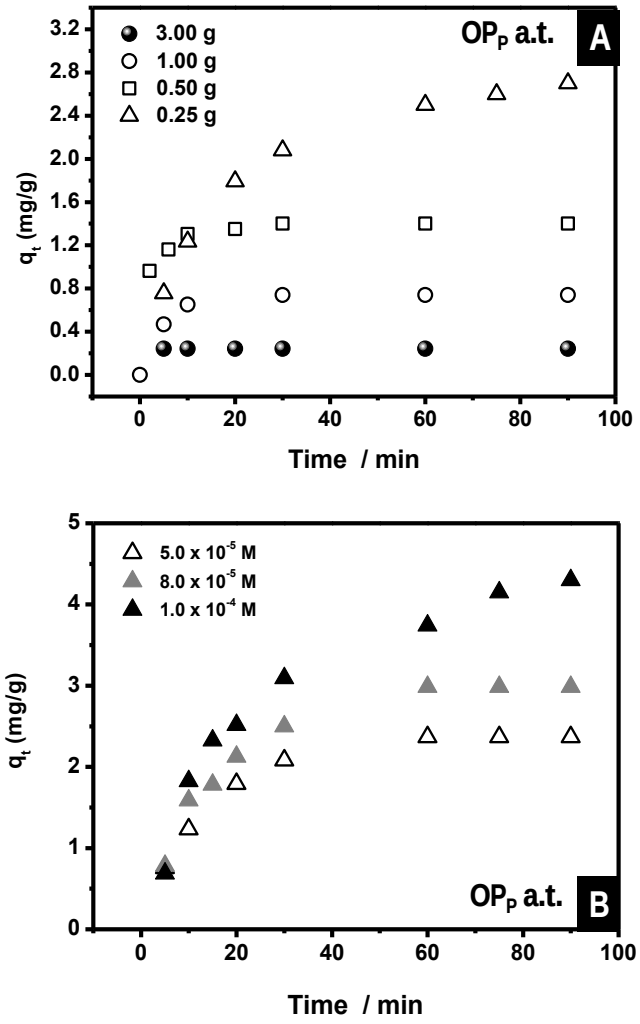

Figure 6: OP_P a.t. amount effect (mg/40 mL dye solution) on the adsorption capacity q_t (mg/g) for DB removal from aqueous/acetic acid (5×10^{-5}M) solutions, pH 3.5 (A); DB concentration effect, at a OP_P a.t. fixed amount (0.25g), on the adsorption capacity q_t (mg/g) for dyes molecules removal from aqueous/acetic acid (5×10^{-5}M) solutions, pH 3.5 (B)

As expected, the percentage of dye removal, at a proper contact time, increased with the increasing of the OP_P a.t. amount and this behavior can be attributed to the increased surface area and the availability of more adsorption sites. More specifically, as usually suggested by several paper reported in literature and related to similar studies[52], the adsorption sites at high adsorbent dosages were not saturated determining the increase of the DB adsorption percentage on olive

pomace. Not surprisingly, the effect resulted to be stronger when OP_P a.t. was considered (Table S4). Results were in excellent agreement with those obtained increasing the DB concentration (Table S5). Indeed, in order to obtain the same efficiency (100%) in dye removal from wastewater, more time was necessary if DB concentration was increased.

It is worth nothing that in order to appreciate variations, measurements were performed using the smallest amount of adsorbent material *i.e* 0.25mg/40mL. Table S5 shows results related to OP_P a.t., however the same considerations can be applied to OP a.t. Regarding the evaluation of q_t values, Figure 6B shows that the maximum adsorption percentage was reached quickly, after few minutes, when a small amount of dye was employed. On the other hand, increasing the dye concentration, more time was necessary to obtain the same efficiency (100%) in dye removal from water. Moreover, the amount of dye adsorbed per unit weight of adsorbent material increased with the increasing of the initial dye concentration and, as suggested by Gercel *et al*.,[60] the higher dye concentration resulted in higher driving force of the concentration gradient. Additionally, under these conditions, the number of collisions between dye and adsorbents increased.[61] This driving force accelerated the diffusion of dyes from the solution into the adsorbent increasing the q_t values.[60] A similar trend was observed for the removal of similar disperse dyes using palm ash or in several different studies reported as references in Ref. 60.

However, from a kinetic point of view, as arise observing the plateaus reported in Figure 6B, the contact time necessary to remove completely the dye, is reduced decreasing the DB concentration in accordance with the availability of more adsorption sites. Differences between OP a.t. and OP_P a.t. were better emphasized reducing the total amount of the adsorbent material (Table S4). After this assessment the q_t values were calculated both for OP a.t. and OP_P a.t., and those related to OP_P a.t. are shown in Figure 6A (the same trend was observed for OP a.t. yet elapsing the contact time). As expected, the percentage of dye removal, at a proper contact time, increased with the increasing of the OP_P a.t. amount and this behavior can be attributed to the increased surface area and the availability of more adsorption sites. More specifically, as usually suggested by several paper

reported in literature and related to similar studies,[52] the adsorption sites at high adsorbent dosages were not saturated determining the increase of the DB adsorption percentage on olive pomace. Not surprisingly, the effect resulted to be stronger when OP_P a.t. was considered (Table S4). Results were in excellent agreement with those obtained increasing the DB concentration (Table S5). Indeed, in order to obtain the same efficiency (100%) in dye removal from wastewater, more time was necessary if DB concentration was increased.

It is worth nothing that in order to appreciate variations, measurements were performed using the smallest amount of adsorbent material i.e 0.25mg/40mL. Table S5 shows results related to OP_P a.t., however the same considerations can be applied to OP a.t. Regarding the evaluation of q_t values, Figure 6B shows that the maximum adsorption percentage was reached quickly, after few minutes, when a small amount of dye was employed. On the other hand, increasing the dye concentration, more time was necessary to obtain the same efficiency (100%) in dye removal from water. Moreover, the amount of dye adsorbed per unit weight of adsorbent material increased with the increasing of the initial dye concentration and, as suggested by Gercel et al. (2008),[60] the higher dye concentration resulted in higher driving force of the concentration gradient. Additionally, under these conditions, the number of collisions between dye and adsorbents increased.[61] This driving force accelerated the diffusion of dyes from the solution into the adsorbent increasing the qt values.[60] A similar trend was observed for the removal of similar disperse dyes using palm ash or in several different studies reported as references in Gercel et al. (2008).[60]

However, from a kinetic point of view, as arise observing the plateaus reported in Figure 6B, the contact time necessary to remove completely the dye, is reduced decreasing the DB concentration in accordance with the availability of more adsorption sites.

3.6 Effect of pH

More details about the nature of interaction between DB and olive pomace were searched changing the pH of dye-containing solution. Experiments were conducted in absence and in the presence of

acetic acid obtaining pH values of 3.5 and 6.6 units. The effect of basic solution was also evaluated, washing OP_P a.t. with an appropriate volume of a basic solution (NaOH), successively dried at 100°C.

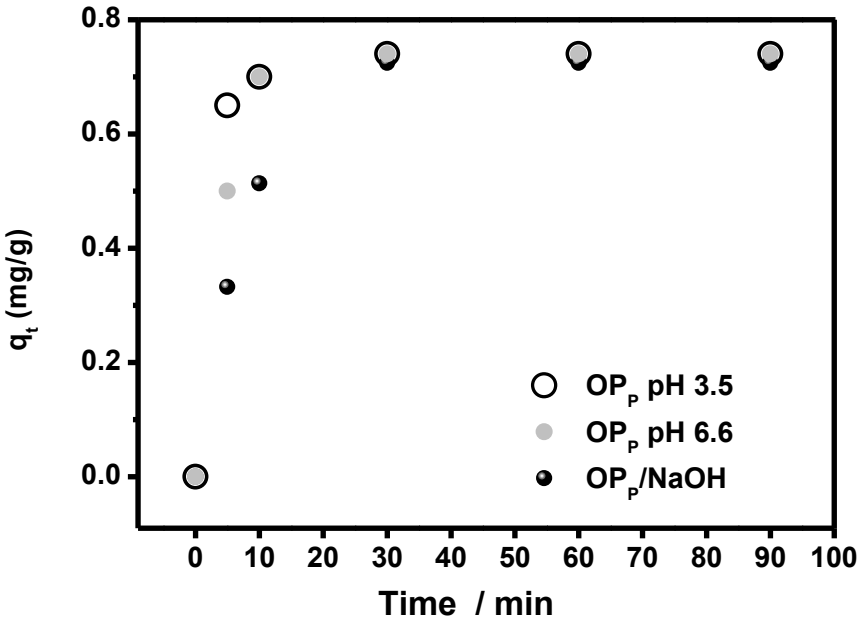

Figure 7: pH value effect on the adsorption capacity q_t (mg/g) of DB removal from aqueous (5×10^{-5}M) solutions, at fixed OP_P a.t. amount (0.25g).

The results are reported in Figure 7 and clearly, if on one hand slight variation was observed changing the pH from 3.5 to 6.6 units, on the other hand significant changes were observed using OP_P a.t. washed with NaOH. As better explained by Isa et al. (2007)[52] the pH values of solution affect both adsorbents surface binding sites and aqueous chemistry of dye. Decreasing the solution pH values, the positive charges control the adsorbent surface and then an electrostatic attraction exists between the positively charged surface of the adsorbent and DB. In our case slight interaction dipole-charge-like could be suggested, considering both the negatively delocalized charge presents on anthraquinone residue and the dipole of ketons. This attractive force increases the adsorption of dye molecules onto the adsorbent surface. When the pH of the system was further increased, the surface of the adsorbent tended to become negatively charged, avoiding the adsorption of disperse

dyes due to the electrostatic repulsion. However it is worth mentioning that, nonetheless the delayed dye adsorption when the OP_P a.t. surface was negatively charged, the adsorption can be still considered excellent, indicating that the electrostatic interactions were not the only types of interaction forces involved in the phenomenon. The presence of Van der Waals, hydrophobic interactions and H-bonds could be considered predominant.

3.7 Kinetic treatments

Interestingly, the dynamics of the adsorption process can be better understood by the evaluation of kinetic data. Indeed, the latter offer useful information on the adsorption process mechanism. In accordance with several studies reported in literature, the adsorption kinetics were interpreted using the first-order and second-order kinetic models by fitting the experimental data with Equations 2 and 3. As shown in Figures 8A and B, the adsorption of DB dye on olive pomace follows a pseudo-second-order kinetics, with excellent regression coefficients (R^2~1) and not the pseudo-first order one. In the latter, the obtained regression coefficients (data not shown) resulted less than 0.99 values (R^2<<0.99). Indeed, usually the pseudo-first order model is not a good fit and fails to predict the amount of dye adsorbed. The linearization were performed also for dye diluted solutions emphasizing again the main role played by the DB concentration (Figure 8B).

3.8 Cycle of adsorption and desorption of dye molecules

Experiments were also performed for evaluating the ability of loaded olive pomace in the DB uptake from wastewater during various adsorption cycles. Table 1 shows the obtained results related both to OP a.t. and to OP_P a.t. Excellent results were obtained after 5 consecutive cycles of DB adsorption from aqueous/acetic acid solution (5×10^{-5}M, pH 3.5). If on one hand the efficiency in dye uptake occurred to be the same when OP_P a.t was considered, on other hand variations were obtained if OP a.t. was studied. It is worth mentioning that the adsorption cycles can be continued.

CYCLE	OP a.t.		OP_P a.t.	
	Efficiency (%)	**Time (min)**	**Efficiency (%)**	**Time (min)**
1	**100**	**120**	**100**	**10**
2	**100**	**300**	**100**	**10**
3	**100**	**300**	**100**	**10**
4	**100**	**300**	**100**	**10**
5			**100**	**10**

Table 1: Effect of consecutive cycles of adsorption of DB at concentration of 5×10^{-5}M, at a fixed amount of OP_P a.t. (0.25 g) and OP a.t. (1.00g), on contact time enough to ensure the complete uptake of DB molecules from aqueous/acetic acid solutions (Volume: 40mL, pH 3.5)

These results highlight the fashionable performance of OP_P a.t. that was further emphasized when adsorption/desorption cycles were considered.

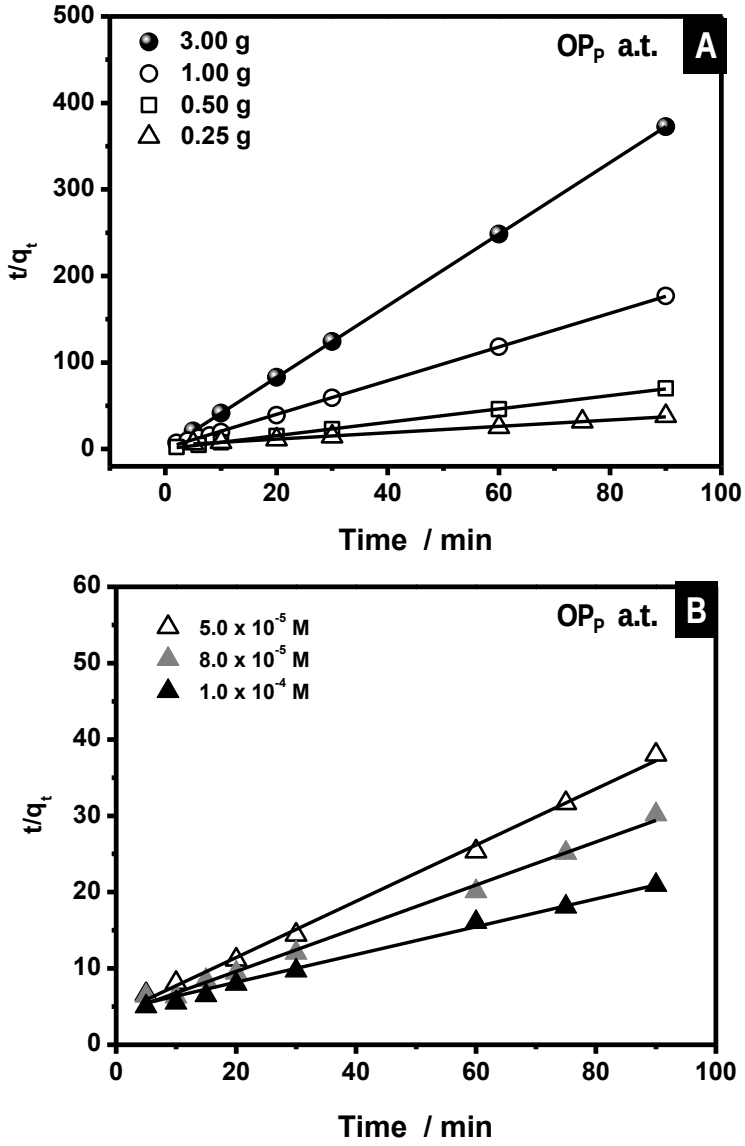

Figure 8: Pseudo-second-order kinetics related to DB removal from pH 3.5 aqueous/acetic acid (5×10^{-5}M) solutions, at several OP_P a.t. amounts (A); pseudo-second-order kinetics related to DB removal from aqueous/acetic acid solution, at several dye concentrations, containing a fixed amount of OP_P a.t. (40 mL, OP_P a.t: 0.25 g, pH 3.5) (B).

3.9 Desorption studies

Several experiments were performed in order to find the best condition to desorb and reuse dye from olive waste. First of all, the pH effect was evaluated. An appropriate amount of OP a.t./DB and/or OP_P a.t./DB was placed in a vessel in contact with aqueous solution having different pH values in the range 2-12. In these conditions the dye release did not occurred. Once again this result

emphasized the scarce role played by the electrostatic interactions in the adsorption phenomenon. Subsequently, organic solvents were adopted and, among them, glacial acetic acid, at room temperature, appeared to be the best one. In fact, after the desorption of the dye, the olive pomace was further reused and subjected to several consecutive cycles of adsorption/desorption. The results, after 5 cycles, are reported in Table 2 showing the efficiency in dye adsorption and desorption with the corresponding contact time.

CYCLE		OP_P a.t.		OP a.t.	
		Efficiency (%)	**Time (min)**	**Efficiency (%)**	**Time(h)**
1	**ADSORPTION**	**100**	**10**	**100**	**2**
	DESORPTION	**78**	**60**	**30**	**2**
2	**ADSORPTION**	**100**	**15**	**100**	**6**
	DESORPTION	**87**	**60**	**30**	**2**
3	**ADSORPTION**	**100**	**30**		
	DESORPTION	**87**	**60**		
4	**ADSORPTION**	**100**	**30**		
	DESORPTION	**78**	**60**		
5	**ADSORPTION**	**100**	**30**		
	DESORPTION	**67**	**180**		

Table 2: Experiments of adsorption/desorption of DB at concentration of 5×10^{-5}M, at a fixed amount of OP_P a.t. (0.25g) and OP a.t. (1.00g), on contact time enough to ensure the complete uptake or the quite recover of DB molecules from aqueous/acetic acid solutions (Volume: 40mL, pH 3.5)

It is worth mentioning that, as for OP_P a.t., the cycles can be continued. Generally the use of OP a.t. appeared not encouraged both for the worst performance and contact time. On the other hand the use of OP_P a.t. ensured a very fast adsorption of dye, ranging from 10 to 30 minutes, with a reasonable desorption time ranging from 60 to 180 minutes, with a mean efficiency of ca. 80% in

dye recover for each cycle. Interestingly, the DB absorption spectrum, after the desorption in acetic acid, occurred to be the same of the one reported in Figure 2B. These results suggested that the dye properties were not changed and its degradation did not occurred, under our experimental conditions. As suggested by Ip et al.,[62] the adsorption reversibility is depended only on weak binding forces present between the DB molecules and olive pomace surface. The weak interactions such as Van der Waals attraction and π-π interactions seem to be dominant and control the adsorption on olive pomace.[62]

4. Conclusions

The synergic use of two spectroscopic techniques (UV-Vis, FTIR-ATR) and SEM, TGA, XPS analyses enabled a careful study related to Disperse Blue 73 removal from wastewater adopting olive pomace as adsorbent material. In order to remove adhering dirt and soluble impurities, when received, OP was washed with hot water (100°C) for several cycles until clean water was obtained (OP a.t.). As a preliminary step of this work, the olive pomace characterization, useful to detail the nature of interaction between DB and olive pomace, was checked adopting several complementary techniques such as SEM, XPS, FTIR-ATR and TG analyses. From SEM analysis a material rich in pores was observed in turn, potentially, able to host the DB molecules. FTIR-ATR and TG analyses suggested the presence of lignin, celluloses and hemicelluloses as the main components of olive pomace and these results were further emphasized by XPS analysis. Afterward, the efficiency on dye removal from wastewater was tested for OP a.t. and, in order to increase the surface area, the powdered OP a.t. (OP_P a.t) was also studied. UV-Visible spectroscopy was used to quantify the amount of adsorbed dye. As expected, excellent results were obtained when OP_P a.t was considered. The effect of several parameters, such as the DB solution pH, the adsorption temperature, the olive pomace and DB amounts, on adsorption process were evaluated. The results show the dependence of adsorption process both on the amount of olive pomace and dye obtaining excellent results at 100°C in the pH range of 3-7 units. An endothermic process was thus presented. The same so far

listed techniques were adopted to evaluate the nature of interaction between DB and olive pomace. FTIR-ATR and XPS analyses suggest the presence of interaction predominantly involving Van der Waals forces and H-bonds between lignin, cellulose and hemicellulose and DB molecules, with a slight contribute of electrostatic interactions. It is worth mentioning that some experiments (data not shown) were also performed completely removing the lignin from olive pomace (by means of oxidation processes) and the obtained results, in terms of dye uploading, occurred to be quite similar to those presented in the paper. So, this indicates that cellulose and cellulose-like structures mainly affected the adsorption process with the large contribute of the material porous structure. Last but not least, interesting results were obtaining when the DB desorption was evaluated. Indeed, glacial acetic acid (solvent used in the textiles dyeing processes), at room temperature, occurred as the most powerful solvent for this purpose enabling the possibility to reuse the adsorbent material for several adsorption/desorption cycles and also for the DB dye recovery potentially usable for other textiles dyeing processes. It is worth mentioning that the dyeing processes occurred at high temperature, thus the excellent performance obtained at 100°C makes olive pomace as a precious agricultural waste useful to treat the industrial disperse dyes-rich hot wastewater.

Acknowledgements

We gratefully acknowledge the skillful and excellent technical assistance of Mr. Sergio Nuzzo and the precious collaboration of Prof. Luisa De Cola, Dr. Eko Adi Prasetyanto and Dr. Pengkun Chen for XPS, TGA and SEM measurements (University of Strasbourg (France), Institut de Science et d'Ingénierie Supramoléculaires)

References

[1] S.P. Buthelezi, A.O. Olaniran, B. Pillay, Textile Dye Removal from Wastewater Effluents Using Bioflocculants Produced by Indigenous Bacterial Isolates. Molecules 17 (2012) 14260-14274.

[2] P.K. Malik, Dye removal from wastewater using activated carbon developed from sawdust: adsorption equilibrium and kinetics, J. Hazard. Mater. 113 (2004) 81-88.

[3] C. Namasivayam, D. Kavitha, Removal of Congo Red from water by adsorption onto activated carbon prepared from coir pith, an agricultural solid waste, Dyes Pigm. 54 (2002) 47-58.

[4] G. Moussavi, M. Mahmoudi, Removal of azo and anthraquinone reactive dyes from industrial wastewaters using MgO nanoparticles, J. Hazard. Mater. 168 (2009) 806-812.

[5] K.S. Bharathi, S.T. Ramesh, Removal of dyes using agricultural waste as low-cost adsorbents: a review, Appl. Water Sci. 3 (2013) 773-790.

[6] C. Dollendorf, S.K. Kreth, S.W. Choi, H. Ritter, Polymerization of novel methacrylated anthraquinone dyes, Beilstein J. Org. Chem. 9 (2013) 453-459.

[7] H. Wang, Q. Li, N. He, Y. Wang, D. Sun, W. Shao, K. Yang, Y. Lu, Removal of anthraquinone reactive dye from wastewater by batch hydrolytic-aerobic recycling process, Sep. Purif. Technol. 67 (2009) 180-186.

[8] P. Semeraro, V. Rizzi, P. Fini, S. Matera; P. Cosma, E. Franco, R. García, M. Ferrandiz, E. Núnez, J.A. Gabaldon, I. Fortea, E. Perez, Interaction between industrial textile dyes and cyclodextrins, Dyes Pigm., 119 (2015) 84-94.

[9] V. Rizzi, A. Longo, P. Fini, P. Semeraro, P. Cosma, E. Franco, R. García, M. Ferrandiz, E. Núnez, J.A. Gabaldon, I. Fortea, E. Perez, Applicative Study (Part I): The Excellent Conditions to Remove in Batch Direct Textile Dyes (Direct Red, Direct Blue and Direct Yellow) from Aqueous Solutions by Adsorption Processes on Low-Cost Chitosan Films under Different Conditions, Adv. Chem. Eng. Sci. 4 (2014) 454-469.

[10] I.K. Kapdan, F. Kargi, Simultaneous biodegradation and adsorption of textile dyestuff in an activated sludge unit, Process Biochem., 37 (2002) 973-981.

[11] A. Bhatnagar, F. Kaczala, W. Hogland, M. Marques, C.A. Paraskeva, V.G. Papadakis, M. Sillanpää, Valorization of solid waste products from olive oil industry as potential adsorbents for water pollution control-a review, Environ. Sci. Pollut. Res. 21 (2014) 268-298.

[12] K. Valta, E. Aggeli, C. Papadaskalopoulou, V. Panaretou, A. Sotiropoulos, D. Malamis, K. Moustakas, K.J. Haralambous, Adding Value to Olive Oil Production Through Waste and Wastewater Treatment and Valorisation: The Case of Greece, Waste Biomass Valorization 6 (2015) 913-925.

[13] A. Roig, M.L. Cayuela, M.A. Sanchez-Monedero, An overview on olive mill wastes and their valorisation methods, Waste Managem. 17 (2012) 960-969.

[14] M.A. Martín-Lara, F. Pagnanelli, S. Mainelli, M. Calero, L. Toro, Chemical treatment of olive pomace: Effect on acid-basic properties and metal biosorption capacity, J. Hazard. Mater. 156 (2008) 448-457.

[15] N.N. Nassar, A. Laith, L.A. Ararb, N. Nedal, N.N. Mareia, M.M. Abu Ghanimb, S. Marwan, M.S. Dwekatb, H. Shadi, S.H. Sawalha, Treatment of olive mill based wastewater by means of magnetic nanoparticles: Decolourization, dephenolization and COD removal, Environ. Nanotechnol. Monitor. Managem. 1-2 (2014) 14-23.

[16] F. Vegliò, F. Beolchini, M. Prisciandaro, Sorption of copper by olive mill residues, Wat. Res. 37 (2003) 4895-4903.

[17] M.A. Martín-Lara, F. Hernáinz, M. Calero, G. Blázquez, G. Tenorio, Surface chemistry evaluation of some solid wastes from olive-oil industry used for lead removal from aqueous solutions, Biochem. Eng. J. 44 (2009) 151-159.

[18] T. Akar, I. Tosuna, Z. Kaynak, E. Ozkara, O.Yeni, E.N. Sahin, S.T. Akar, An attractive agro-industrial by-product in environmental cleanup: Dye biosorption potential of untreated olive pomace, J. Hazard. Mater. 166 (2009) 1217-1225.

[19] S.H. Gharaibeh, W.Y. Abu-El-Shar, M.M. Al-Kofahi, Removal of selected heavy metals from aqueous solutions using processed solid residue of olive mill products, Wat. Res. 32 (1998) 498-502.

[20] F. Pagnanelli, L. Toro, F. Vegliò, Olive mill solid residues as heavy metal sorbent material:a preliminary study, Waste Mangem. 22 (2002) 901-907.

[21] F. Pagnanelli, S. Mainelli, F. Vegliò, L. Toro, Heavy metal removal by olive pomace: biosorbent characterization and equilibrium modelling, Chem. Eng. Sci. 58 (2003) 4709-4717.

[22] A. Hawari, Z. Rawajfih, N. Nsour, Equilibrium and thermodynamic analysis of zinc ions adsorption by olive oil mill solid residues, J. Hazard. Mater. 168 (2009) 1284-1289.

[23] Y. Nuhoglu, E. Malkoc, Thermodynamic and kinetic studies for environmentaly friendly Ni(II) biosorption using waste pomace of olive oil factory, Bioresour. Technol. 100 (2009) 2375-2380.

[24] A. Hawari, M. Khraisheh, A. Mohammad, M.A. Al-Ghouti, Characteristics of olive mill solid residue and its application in remediation of Pb^{2+}, Cu^{2+} and Ni^{2+} from aqueous solution: Mechanistic study, Chem. Eng. J. 251 (2014) 329-336.

[25] M. Uğurlu, A. Gürses, Ç. Doğar, Adsorption studies on the treatment of textile dyeing effluent by activated carbon prepared from olive stone by ZnCl2 activation, Col. Technol. 123 (2007) 106-114.

[26] S. Hemsas, H. Lounici, Z. Belkebi, Khaled Benrachedi, Removal of Dispersed Dyes from Aqueous Solution Using Activated Carbon Prepared from Olive Stones, J. Agric. Sci. Technol. A 4 (2014) 414-421.

[27] G. Cimino, R.M. Cappello, C. Caristi, G. Toscano, Characterization of carbons from olive cake by sorption of wastewater pollutants, Chemosphere 61 (2005) 947-955.

[28] W.Y. Abu-El-Shar, S.H. Gharaibeh, S. Mahmoud, Removal of dyes from aqueous solutions using low-cost sorbents made of solid residues from olive-mill wastes (JEFT) and solid residues from refined Jordanian oil shale, Environ. Geol. 39 (2000) 1090-1094.

[29] E.A. El-Sharkawy, A.Y. Soliman, K.M. Al-Amer, Comparative study for the removal of methylene blue via adsorption and photocatalytic degradation, J. Colloid Interface Sci. 310 (2007) 498-508.

[30] J.H. Ramirez, F.J. Maldonado-Hodar, A.F. Perez-Cadenas, C. Moreno-Castilla, C.A. Costa, L.M. Madeira, Azo-dye Orange II degradation by heterogeneous Fenton-like reaction using carbon-Fe catalysts, Appl. Catal. B. 75 (2007) 312-323.

[31] P. Pala, E. Galiatsatou, H. Tokat, C. Erkaya, C. Israilides, D. Arapoglou, The Use of Activated Carbon from Olive Oil Mill Residue, for the Removal of Colour from Textile Wastewater, European Water 13/14 (2006) 29-34.

[32] R. Baccar, P. Blánquez, J. Bouzid, M. Feki, M. Sarrà, Equilibrium, thermodynamic and kinetic studies on adsorption of commercial dye by activated carbon derived from olive-waste cakes, Chem. Eng. J. 165 (2010) 457-464.

[33] I. Demiral, Methylene blue adsorption from aqueous solution using activated carbon prepared from olive bagasse, Fresenius Environ. Bull. 20 (2011) 127-134.

[34] M. Berrios, M.Á. Martín, A. Martín, Treatment of pollutants in wastewater: adsorption ofmethylene blue onto olive-based activated carbon, J. Ind. Eng. Chem. 18 (2012) 780-784.

[35] F. Banat, S. Al-Asheh, R. Al-Ahmad, F. Bni-Khalid, Bench-scale and packed bed sorption of methylene blue using treated olive pomace and charcoal, Bioresour. Technol. 98 (2007) 3017-3025.

[36] I. Anastopoulos, I. Massas and C. Ehaliotis, Use of residues and by-products of the olive-oil production chain for the removal of pollutants from environmental media: A review of batch biosorption approaches, J. Environ. Sci. Health. 50 (2015) 677-718.

[37] G. McKay, Y.S. Ho, Pseudo-second order model for sorption processes, Process. Biochem. 34 (1999) 451-465.

[38] M. Anbia, S. Asl Hariri, Removal of methylene blue from aqueous solution using nanoporous SBA-3, Desalination 261 (2010) 61-65.

[39] M.A. Ahmad, N.A.A. Puad, O.S.Bello, Kinetic, equilibrium and thermodynamic studies of synthetic dye removal using pomegranate peel activated carbon prepared by microwave-induced KOH activation, Water Research and Industry 6 (2014) 18-35.

[40] T.W. Seow, C.K. Lim, Removal of Dye by Adsorption: A Review, Int. J. Appl. Eng. Res. 11 (2016) 2675-2679.

[41] S. Senthilkumaar, P. Kalaamani, C.V. Subburaam, Liquid phase adsorption of crystal violet onto activated carbons derived from male flowers of coconut tree, J. Hazard. Mater. 136 (2006) 800-808.

[42] A.A. Rajabi, Y. Yamini, M. Faraji, F. Nourmohammadian, Modified magnetite nanoparticles with cetyltrimethylammonium bromide as superior adsorbent for rapid removal of the disperse dyes from wastewater of textile companies, Nano. Chem. Res. 1 (2016) 49-56.

[43] S.H. Etaiw, M.M. Abou-Sekkina, G.B. El-Hefnawey, S.S. Assar, Studies on Azo Compounds: Part V-Spectrophotometric Studies on Some Quinoline Azo Dyes, Indian J. Text. Res. 7 (1982) 19-23.

[44] A.N. Diaz, Absorption and emission spectroscopy and photochemistry of 1,10-anthraquinone derivatives: a review, J. Photochem. Photobiol. 53 (1990) 141-167.

[45] (a) H. Mao, C. Wang and Y. Wang, Synthesis of polymeric dyes based on waterborne polyurethane for improved color stability, New J.Chem. 39 (2015) 3543-3550. (b) H. Mao, F. Yang, C. Wang, Y. Wang, D. Yaob, Y. Yina, Anthraquinone chromophore covalently bonded blocked waterborne polyurethanes: synthesis and application, RSC Adv. 5 (2015) 30631-30639.

[46] A.P. Dahiya, M. Kumbhakar, D.K. Maity, T. Mukherjee, A.B.R. Tripathi, N. Chattopadhyay, H. Palb, Solvent polarity and intramolecular hydrogen bonding effects on the photophysical properties of 1-amino-9,10-anthraquinone dye, J. Photochem. Photobiol. 181 (2006) 338-347.

[47] F.A.S. Chipem, A. Mishra, G. Krishnamoorthy, The role of hydrogen bonding in excited state intramolecular charge transfer, Phys. Chem. 14 (2012) 8775-8790.

[48] S. Pramodini, P. Poornesh, Effect of conjugation length on nonlinear optical parameters of anthraquinone dyes investigated using He–Ne laser operating in CW mode, Opt. Laser Technol. 62 (2014) 12-19.

[49] A. Mousa, G. Heinrich, U. Gohs, R. Hässler, U. Wagenknecht, Application of Renewable Agro-Waste-Based Olive Pomace on the Mechanical and Thermal Performance of Toughened PVC, Polym.-Plast. Technol. Eng. 48 (2009) 1030-1040.

[50] H. A. Omar, L. Abd El -Baset Attia, Kinetic and equilibrium studies of cesium-137 adsorption on olive waste from aqueous solutions, Radiochemistry 55 (2013) 497-504.

[51] S. Timofei, W. Schmidt, L. Kurunczi, Z. Simon, A review of QSAR for dye affinity for cellulose fibres, Dyes Pigm. 47 (2000) 5-16.

[52] M.H. Isa, L.S. Lang, F.A.H. Asaari, H.A. Aziz, N.A. Ramli, J.P.A. Dhas, Low cost removal of disperse dyes from aqueous solution using palm ash, Dyes Pigm. 74 (2007) 446-453.

[53] L.S. Johansson, J.M. Campbell, Reproducible XPS on biopolymers: cellulose studies, Surf. Interface Anal. 36 (2004) 1018-1022.

[54] A. Clemente, R. Sánchez-Vioque, J. Vioque, J. Bautista, F. Millán, Chemical composition of extracted dried olive pomaces containing two and three phases, Food Biotechnol. 11 (1997) 273-291.

[55] B. Sundberg, E. Mellerowicz, P. Persson, XPS study of living tree, Surf. Interface Anal. 34 (2002) 284-288.

[56] V. Rizzi, P. Fini, F. Fanelli, T. Placido, P. Semeraro, T. Sibillano, A. Fraix, S. Sortino, A. Agostiano, C. Giannini, P. Cosma, Molecular interactions, characterization and photoactivity of Chlorophyll a/chitosan/2-HP-b-cyclodextrin composite films as functional and active surfaces for ROS production, Food Hydrocolloids 58 (2016) 98-112.

[57] S.B. Kabakci, H. Aydemir, Pyrolysis of Olive Pomace and Copyrolysis of Olive Pomace with Refuse Derived Fuel, Environ. Prog. Sustainable Energy 33 (2013) 649-656.

[58] M.K. Tawarah, R.A. Rababah, Characterization of Some Jordanian Crude and Exhausted Olive Pomace Samples, Green Sustainable Chem. 3 (2013) 146-162.

[59] M.D. La Rubia-García, Á. Yebra-Rodríguez, D. Eliche-Quesada, F.A. Corpas-Iglesias, A. López-Galindo, Assessment of olive mill solid residue (pomace) as an additive in lightweight brick production, Con. Buil. Mat. 36 (2012) 495-500.

[60] O. Gercel, H.F. Gercel, A. Savas, C. Koparal, U.B. Ogutveren, Removal of disperse dye from aqueous solution by novel adsorbent prepared from biomass plant material, J. Hazard. Mater. 160 (2008) 668-674.

[61] G.O. El-Sayed, M.E. Moustafa, M.F. Mahrous, Removal of Disperse 2BLN Dye from Industrial Water onto Activated Carbon Prepared from Sugar Can Stalks, Int. J. Chem. Tech. Res. 3 (2011) 1604-1611.

[62] A.W.M. Ip, J.P. Barford, G. McKay, Reactive Black dye adsorption/desorption onto different adsorbents: Effect of salt, surface chemistry, pore size and surface area, J. Colloid Interface Sci. 337 (2009) 32-38.

Graphical Abstract

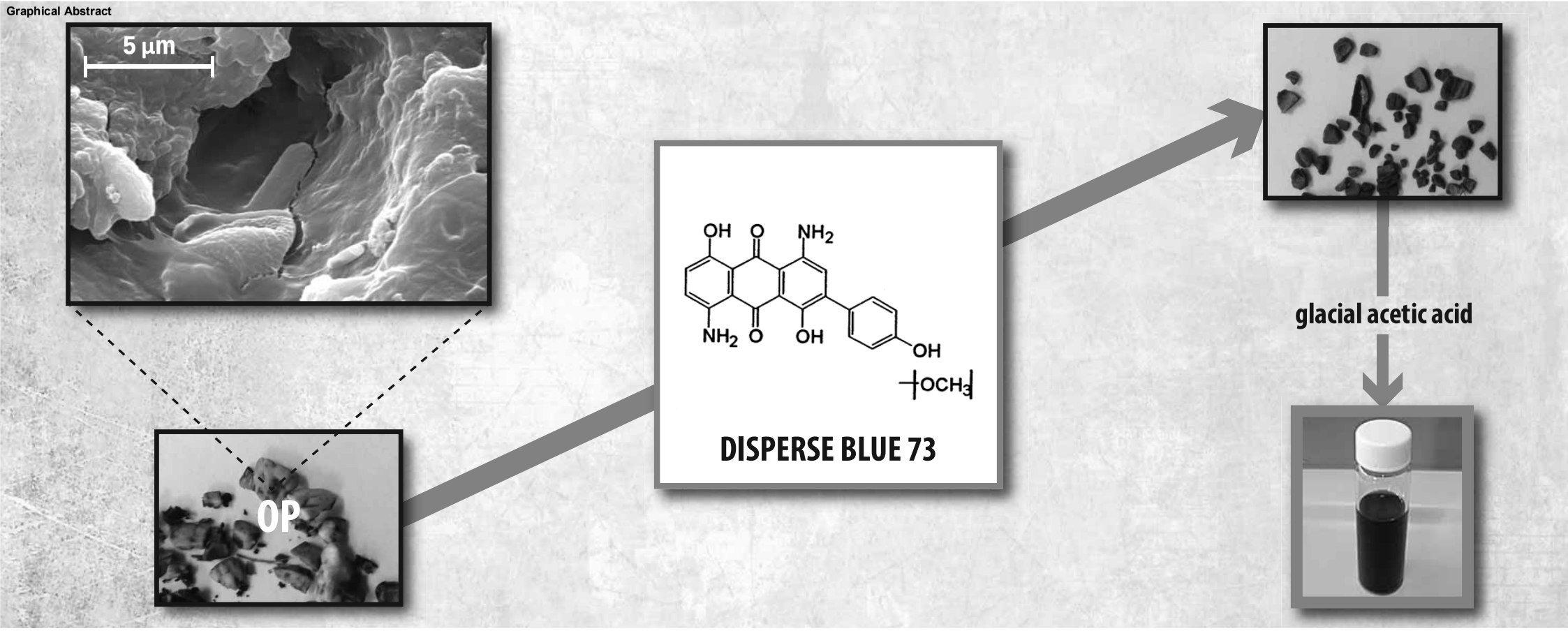

- Olive pomace: an interesting adsorbent material for wastewater cleanup.
- Disperse blue removal and reuse from textile effluents.
- An alternative use of olive pomace reducing globally the pollutants disorder.

Supplementary Interactive Plot Data (CSV)

Click here to download Supplementary Interactive Plot Data (CSV): Electronic Supporting Material v1.0.docx